Journal of Materials Chemistry A

Accepted Manuscript

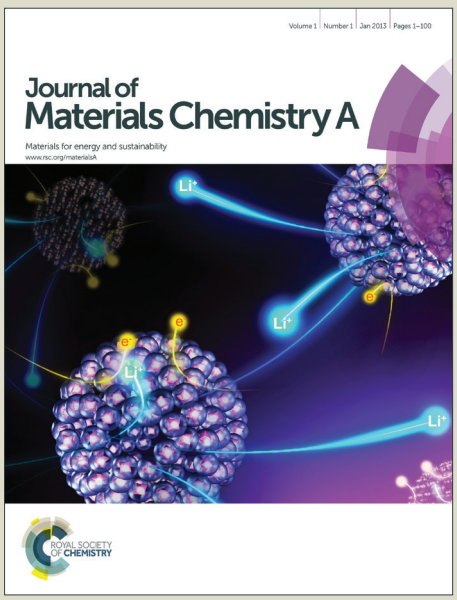

This is an *Accepted Manuscript*, which has been through the Royal Society of Chemistry peer review process and has been accepted for publication.

Accepted Manuscripts are published online shortly after acceptance, before technical editing, formatting and proof reading. Using this free service, authors can make their results available to the community, in citable form, before we publish the edited article. We will replace this *Accepted Manuscript* with the edited and formatted *Advance Article* as soon as it is available.

You can find more information about *Accepted Manuscripts* in the Information for Authors.

Please note that technical editing may introduce minor changes to the text and/or graphics, which may alter content. The journal's standard Terms & Conditions and the Ethical guidelines still apply. In no event shall the Royal Society of Chemistry be held responsible for any errors or omissions in this *Accepted Manuscript* or any consequences arising from the use of any information it contains.

ROYAL SOCIETY OF CHEMISTRY

www.rsc.org/materialsA

Journal of Materials Chemistry A RSCPublishing

ARTICLE

Non-Toxically Enhanced Sulfur Reaction for Chalcogenide Thin Film Using a Thermal Cracker

Cite this: DOI: 10.1039/xoxxoooooox

Dae-Hyung Cho,*[a] Woo-Jung Lee,[a] Sang-Woo Park,[b] Jae-Hyung Wi,[a] Won Seok Han,[a] Jeha Kim,[b] Mann-Ho Cho[c], Dongseop Kim[d] and Yong-Duck Chung[ae]

Received ooth January 2014,
Accepted ooth January 2014

DOI: 10.1039/xoxxoooooox

www.rsc.org/

Sulfur-based metal chalcogenide films have been widely used for high-performance optoelectronic devices due to its attractive optical and electrical properties. Although typical approaches to the chemical deposition of chalcogenide films have some advantages such as large-area coverage and high thickness controllability, these processes require highly toxic and expensive hydrogenated materials. Here, we demonstrate an enhanced sulfur reaction with an environmentally-safe and cost-competitive method using a thermal sulfur cracker cell. The elevated cracking-zone temperature enhanced the reactivity of sulfur by cracking evaporated sulfur molecules into smaller molecules, and yielded the formation of high-quality ZnS phase maintaining low substrate temperature. The fabricated ultra-thin ZnS film played an excellent role as a buffer layer of the $Cu(In,Ga)Se_2$ thin-film solar cell, as the film showed high photovoltaic performances.

Introduction

Interest in metal chalcogenide materials has been continuously growing for various optoelectronic applications such as photovoltaic[1-3], display devices[4], and batteries[5] due to their good electrical and optical properties. The metal chalcogenide compound contains one or more chalcogen elements such as sulfur, selenium, and tellurium, exhibiting semiconducting properties by bonding with transition metal elements. Recently, among metal chalcogenide materials, sulfur-based compounds such as ZnS, MoS_2, CuS, CdS, SnS, $SnS_{2-x}Se_x$, $Cu(In,Ga)(Se,S)_2$, and $Cu_2ZnSn(Se,S)_4$ are being extensively studied because of their high carrier mobility, large band-gap, and good photovoltaic properties.[6-13] Conventionally, among various techniques of fabricating sulfur-based films, atomic layer deposition (ALD), ion-layer gas reaction (ILGAR), chemical bath deposition (CBD), and spin-coating are promising due to their high step-coverage, thickness controllability, and large-area uniformity.[11,14] However, these techniques have some drawbacks. The H_2S gas or hydrazine (N_2H_4) solution, widely used in the ALD, ILGAR, and spin coating methods, are highly toxic and extremely expensive.[15,16] Furthermore, the metal precursor, including a metal element bonded to atomic or molecular ligands, is more expensive than pure metals. On the other hand, the wet processes, such as the CBD and spin-coating, rule out vacuum compatibility. In order to overcome these environmental, cost, and vacuum compatibility issues, we need to use safe, cheap, and solid-state non-ionized materials for the fabrication of the sulfur-based chalcogenide films. However, the metal and sulfur sources are more stable than the ionized forms, which require a high vapor pressure and a great deal of energy (e.g. high-temperature substrate heating) for the reaction between metal and sulfur. The high substrate temperature can raise the manufacturing cost and induce performance degradation when the underlying device is vulnerable to heat.

In this study, we suggest a novel method of enhancing the reactivity of sulfur by applying a great deal of thermal energy into evaporated sulfur molecules with a thermal cracker cell using non-toxic and low-cost materials. Shin *et al* utilized the sulfur cracker for fabrication of $Cu_2ZnSn(S_xSe_{1-x})_4$ light absorber layers.[17,18] We have observed the effect of the thermal sulfur cracker cell on the formation of chalcogenide ZnS thin films and investigated its feasibility for the application for a photovoltaic device. This work offers various advantages of cost-effectiveness, eco-friendliness, and vacuum-compatibility in the manufacturing process of sulfur-based chalcogenide films for optoelectronic devices.

Experimental

ZnS unit layer

The 50-nm-thick Zn film was firstly deposited on the soda-lime glass (SLG) substrate by using a DC-sputtering with a power of 40

Journal of Materials Chemistry A Accepted Manuscript

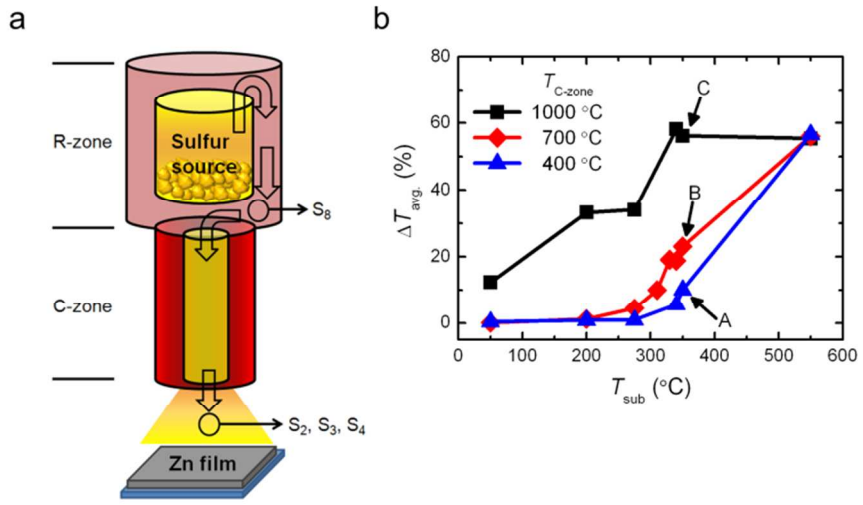

Figure 1. (a) Schematic of the thermal sulfur cracker cell used in this study. (b) The change of the average transmittance ($\Delta T_{avg.}$) of the ZnS thin films prepared on SLG substrates with varying both T_{sub} and $T_{C\text{-zone}}$ at fixed $T_{R\text{-zone}}$ (= 150°C).

W and an Ar working pressure of 90 mTorr at room temperature. A commercial Zn sputter target (TASCO, 99.999% purity) was used. The Zn-deposited sample was successively moved into another vacuum chamber for a sulfur reaction by using the cracker cell. In the sulfur reaction process, $T_{R\text{-zone}}$, base pressure, and working pressure were 150°C, $< 1.0 \times 10^{-6}$ Torr, and $\sim 5.0 \times 10^{-5}$ Torr, respectively. The T_{sub} and $T_{C\text{-zone}}$ were varied at R.T. − 550°C and 400 − 1000°C, respectively. The sulfur source (Cerac) was solid granules with a purity of 99.9%.

The optical transmittance of the ZnS film was observed by a UV−VIS spectrophotometer (Hitachi U−4001). The phase behavior of the sulfur-reacted Zn film was analyzed by a grazing-incident 2θ-ω scan using a multi-purpose X-ray diffractometer (PANalytical, X'pert PRO-MPD). We observed the film morphology using an SEM (FEI, Magellan400). The XPS (ULVAC-PHI, PHI-5000) measurement revealed the chemical states of the ZnS films prepared on the SLG substrates. The XPS spectra of the ZnS films were obtained with Mg *K*α source (1253.6 eV) and pass energy of 20 eV and were repeatedly taken at different time intervals by Ne ion sputtering with an energy of 2 keV.

Application to CIGS thin-film solar cell device

For an application of ZnS to a buffer layer, we fabricated the CIGS thin-film solar cell with a typical Al/Ni/ITO/ZnO/ZnS/CIGS/Mo/SLG structure without an anti-reflection coating using the DC-magnetron sputtered Mo back contact, co-evaporated CIGS, RF-sputtered ITO/ZnO window layer, and e-beam evaporated Al/Ni grid. A 2.3-μm-thick CIGS was deposited via a well-known multi-stage process. A detailed description of the solar cell fabrication can be found elsewhere.[19-21]

The morphology of the very thin ZnS film (~8 nm) was observed using an SEM and a TEM (FEI, Tencai g20). The REELS (VG ESCALAB 210) measurement revealed the energy band-gap of the thin ZnS films prepared on the CIGS film. The REELS spectra were excited with the primary electron energy of 500 and 1780 eV. A secondary ion-mass spectrometer (SIMS, CAMECA IMS 6f) analysis of the 8-nm-ZnS/CIGS sample was carried out using O^{2+} primary ion bombardment included an 200 nA primary current rastered over a 200 μm x 200 μm area with 15 keV impact energy. The XPS spectra of the 8-nm-ZnS/CIGS sample were acquired at different time intervals by Ar ion sputtering with an energy of 1 keV. The *I*−*V* characteristics of the CIGS solar cells were measured using an *I*−*V* source meter (Keithley 2400) under a global Air Mass 1.5 spectrum for 1000 W m^{-2} irradiance at room temperature. Each solar cell was mechanically isolated and the effective area was 0.47 cm^2. The external quantum efficiency was acquired using a spectrally-resolved monochromatic light with a 12 W halogen lamp (PV measurement).

Results and discussion

We used a cracker cell (JMON, SCS-500D) for the sulfur reaction, as shown in Figure 1a.[22-24] The sulfur cracker cell is a layout design of down-pouring sources consisting of a reservoir zone (R-zone, typical Knudsen cell) annexing a thermal cracking zone (C-zone) in series. The vapor phase of sulfur, evaporated from solid-phase granule sources in R-zone (fixed at 150°C), goes thorough C-zone (varied from 400 to 1000°C). At the temperature of 150°C the S_8 molecule is known to dominantly exist in sulfur vapor because the formation enthalpy of S_8 (= 24.32 $kcal_{th}$ mol^{-1}) is smaller than that of S_2, S_3, and S_4 (= 31.20, 33.81, and 34.84 $kcal_{th}$ mol^{-1}, respectively).[25] When sulfur vapor passes through the C-zone, the number of species, such as S_2, S_3, and S_4, rapidly increases above 500°C.[25] This is because a portion of S_8 is cracked into smaller molecules at high temperatures. Thus, the cracked sulfur vapor during a high-temperature treatment at C-zone is believed to greatly enhance the chemical reactivity compared to that of non-cracked sulfur molecular vapor.

Journal of Materials Chemistry A Accepted Manuscript

This journal is © The Royal Society of Chemistry 2012

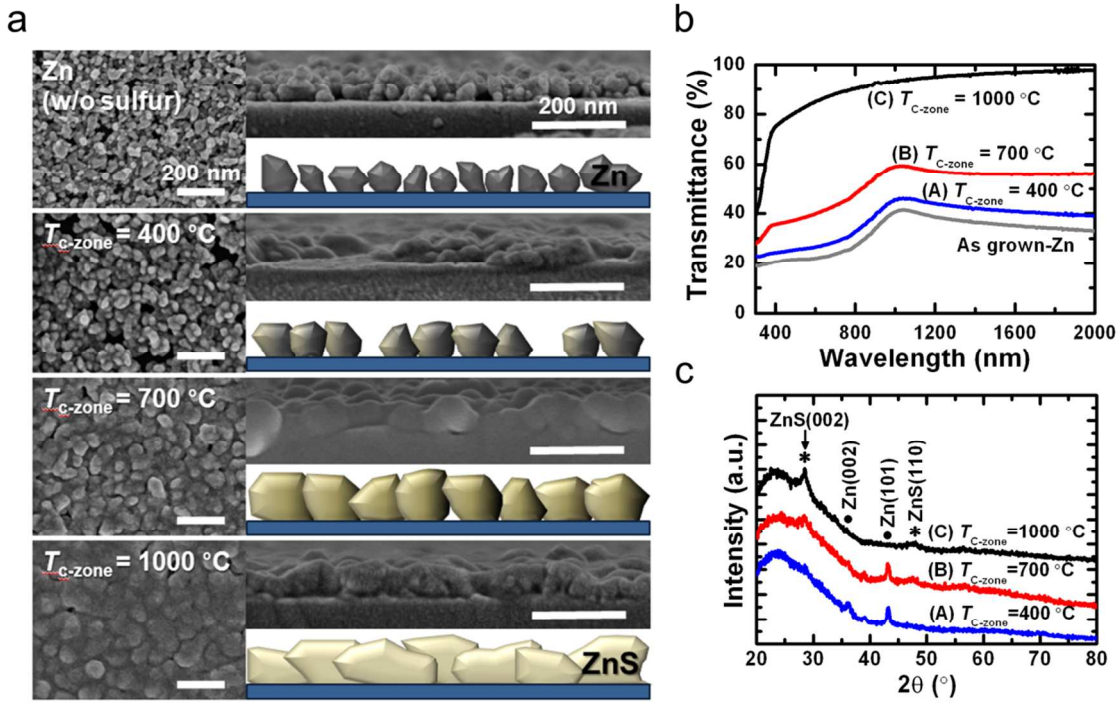

Figure 2. Influence of $T_{C\text{-}zone}$ on physical properties of ZnS films at a fixed T_{sub} of 350°C. (a) SEM top-view and cross-section images, (b) optical transmission spectra, and (c) GIXRD spectra of the Zn films after a sulfur reaction with different $T_{C\text{-}zone}$s of 400°C, 700°C, and 1000°C. The X-ray diffraction patterns were identified as Zn (solid circle) and ZnS (star) by JCPDF 87-0713 and JCPDF 36-1450, respectively.

In order to experimentally observe the effect of the C-zone on the sulfur reaction, we used a Zn metal deposited on the SLG as a reactant precursor and varied the cracking-zone temperature ($T_{C\text{-}zone}$) for the sulfur reaction process. Moreover, we varied the substrate temperature (T_{sub}) from R.T. to 550°C at each $T_{C\text{-}zone}$. An as-grown 50-nm-Zn film showed a relatively low transmittance of ~ 30%, whereas, the transmittance of Zn film increased after the sulfur reaction. The enhancement of transmittance after the sulfur reaction implies the formation of ZnS phase since the semiconducting ZnS film has a bandgap energy at a short wavelength of ~ 360 nm. Figure 1b shows the difference of the average transmittances ($\Delta T_{avg.}$) of ZnS films as a function of $T_{C\text{-}zone}$ and T_{sub}. The $\Delta T_{avg.}$ were obtained by comparing the average transmittances of the film between before and after sulfur reactions in the wavelength range of 400 − 1500 nm. The $\Delta T_{avg.}$ increased at each $T_{C\text{-}zone}$ with increasing T_{sub}. At a $T_{C\text{-}zone}$ of 1000°C, the $\Delta T_{avg.}$ rapidly increased in proportion to T_{sub} and saturated at lower T_{sub} (over 340°C). The observation indicates that ZnS compound formation begins at $T_{sub} \geq$ 340°C and rapidly develops with the cracking temperature at 1000°C. The T_{sub} of 340°C that yielded ZnS formation was much lower than the reported heating temperature over 500°C in sulfurization processes for ZnS films.[26,27] We closely investigated the physical properties of ZnS films grown at T_{sub} = 350°C, indicating remarkable change of the $\Delta T_{avg.}$ as a function of $T_{C\text{-}zone}$, as expressed by A, B, and C in Figure 1b.

Figure 2a shows the planar and cross-sectional SEM images of ZnS film formed at a T_{sub} of 350°C with different $T_{C\text{-}zone}$ of 400°C, 700°C, and 1000°C. Additionally, the morphological characteristic of the sputter-deposited Zn film prior to the sulfur reaction was investigated. The pure Zn film consisted of very small island-shaped grains with diameter sizes of 20 − 40 nm containing a number of voids. This is resulted from the larger surface energy of Zn film (~ 0.99 J m^{-2})[28] than that of a glass substrate (amorphous SiO_2, ~ 0.34 J m^{-2})[29]; *i.e.*, Zn grows in an island shape on glass.[30] At $T_{C\text{-}zone}$ of 400°C, the grain size increased and the void size also became larger. The grains came to agglomerate with the adjacent small grains, enlarging the voids, yet the grain size is still too small to fill up the voids because of the low reactivity of the sulfur. At higher $T_{C\text{-}zone}$ of 700°C and 1000°C, the enhanced reactivity of sulfur expanded the grain size and the voids disappeared. Consequently, as $T_{C\text{-}zone}$ increased, the grain size of ZnS expanded both laterally and vertically and filled up the voids although the final film seemed to be slightly porous. For a better understanding, the schematic images of the ZnS film growth at each $T_{C\text{-}zone}$ condition are illustrated in the inset of Figure 2a. The sulfur reaction at the elevated $T_{C\text{-}zone}$ is an effective void-filling process converting the void-containing island-shaped grains into the void-free dense film.

The optical, structural, and chemical properties of the sulfur-reacted Zn films were investigated. The optical transmittance of ZnS films increased with increasing $T_{C\text{-}zone}$ in the whole range of wavelength (300 − 2000 nm) as shown in Figure 2b. The ZnS film formed above a $T_{C\text{-}zone}$ of 700°C exhibited a sharp kink of the spectra near the band-gap energy (< 400 nm). The optical band-gap energy of ZnS film with $T_{C\text{-}zone}$ = 1000°C was estimated to 3.40 eV from a Tauc plot.

Journal of Materials Chemistry A Accepted Manuscript

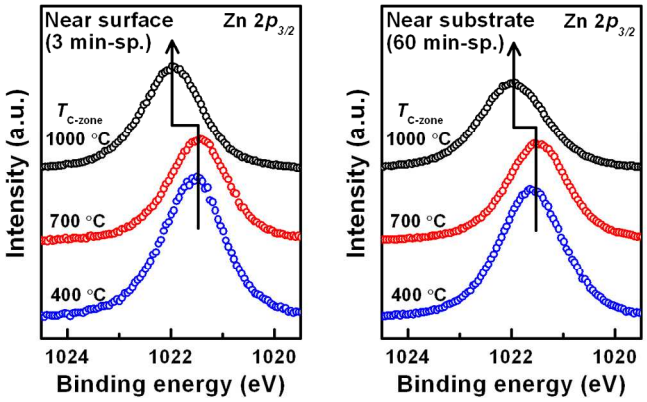

Figure 3. XPS spectra near Zn $2p_{3/2}$ of the Zn films after a sulfur reaction with different $T_{C\text{-zone}}$s of 400°C, 700°C, and 1000°C measured at different sputter etching times of 3 and 60 min.

The grazing incidence X-ray diffraction (GIXRD) result was shown in Figure 2c. As increasing $T_{C\text{-zone}}$, the diffraction peak of ZnS (002) phase emerged while the both peaks of Zn (101) and Zn (002) phase decreased. The ZnS film with $T_{C\text{-zone}}$ = 1000°C (C) showed only the ZnS phases with the strong (002)-orientated texture, which is consistent with the transmittance result of Figure 2b.

Figure 3 shows the XPS spectra of Zn $2p_{3/2}$ peaks at different depths of the film with sputtering times of 3 min and 60 min, with varying $T_{C\text{-zone}}$. The spectra obtained at 3 min-sputter time indicate the chemical states near surface of the film with a removal of the carbon contamination, while the spectra acquired at 60 min-sputter time indicate the information near interface between film and substrate. At both the sputtering times of 3 min and 60 min, the Zn $2p_{3/2}$ peaks shifted from binding energies assigned to Zn (~ 1021.5 eV)[31] to higher energies for ZnS (~ 1022.0 eV)[32,33] at $T_{C\text{-zone}}$ of 1000°C. This result suggests that the ZnS film was completely formed at the high $T_{C\text{-zone}}$ of 1000°C while the unreacted Zn phase remained up to $T_{C\text{-zone}}$ of 700°C. The intensity and position of S 2*p* peak showed little change as a function of both the $T_{C\text{-zone}}$ and sputtering time as shown in Figure S1.

Table 1. Cell parameters of the CIGS solar cells at various ZnS thicknesses from 0 to 30 nm.

t_{ZnS} (nm)	PCE (%)	V_{OC} (V)	J_{SC} (mA cm^{-2})	*FF* (%)
0	3.99	0.369	28.81	37.4
8	7.97	0.435	32.89	55.7
15	3.62	0.419	17.51	49.4
20	2.36	0.420	10.97	51.3
30	0.19	0.119	4.12	39.2

We fabricated the Cu(In,Ga)Se_2 (CIGS) thin-film solar cells with a structure of Al/Ni/ITO/ZnO/ZnS/CIGS/Mo/SLG, as shown in Figure 5a, to verify the feasibility of the cracker-ZnS buffer layer for a photovoltaic application. The thickness of the ZnS layer (t_{ZnS}) was varied from 0 to 30 nm using different Zn thicknesses. Table 1 shows photovoltaic performance parameters including the power

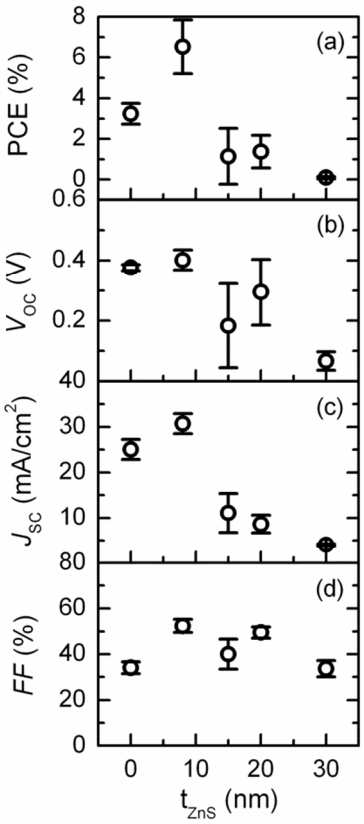

Figure 4. Solar cell performance parameters, including the (a) PCE, (b) V_{OC}, (c) J_{SC}, and (d) *FF* of the CIGS photovoltaic devices, as a function of Zn thickness. Six cells were fabricated at each Zn thickness. The error bars indicate standard errors of mean.

conversion efficiency (PCE), open-circuit voltage (V_{OC}), short-circuit current density (J_{SC}), and fill factor (*FF*) of one of the best PCEs at each t_{ZnS}. A PCE of 7.97% was achieved at a t_{ZnS} of 8 nm, which was largely improved compared with the solar cell without a buffer (3.99%). The 8-nm-ZnS successfully formed a *p-n* junction with the CIGS. However, as t_{ZnS} increased, the PCE rapidly decreased, mainly due to the J_{SC} drop. The calculated series resistances (R_S) of the solar cells dramatically increased with an increase in the thickness because the R_S increased monotonically from 1.09 to 4.90 Ωcm^2 with the thickness of 8 to 30 nm. The large R_S hinders the electron transport through the cell.[34] The R_S was obtained by fitting *I-V* curves in a two-diode model.[35] The statistical performance data with error bars are shown in Figure 4.

The *J-V* curve and EQE spectrum of the best cell were plotted in Figures 5b and c. The best PCE of 12.6% with V_{OC} = 0.504 V, J_{SC} = 37.40 mA cm^{-2}, and *FF* = 66.80% was obtained using both the 8-nm-ZnS and the optimized ZnO/ITO window layer. The experimental detail for optimization of ZnO and ITO processes is described in the Supporting Information. The EQE spectrum exhibited a relatively high intensity in the short-wavelength region (300 − 500 nm), which yielded high J_{SC} compared with that of the CdS-buffered solar cells.[36,37]

Journal of Materials Chemistry A Accepted Manuscript

This journal is © The Royal Society of Chemistry 2012

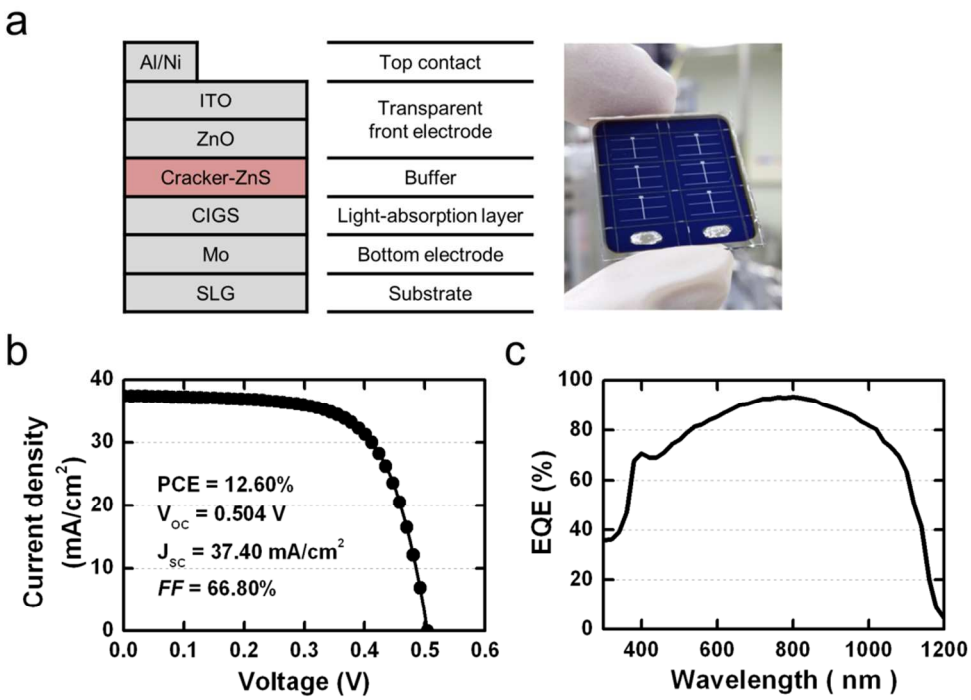

Figure 5. Application of the ultra-thin ZnS film to the CIGS thin-film solar cell. (a) Illustration of the fabricated structure of CIGS solar cell and the role of each layer and photograph of a fabricated solar cell sample. (b) *J-V* curve and (c) quantum efficiency of the best CIGS solar cell with an 8-nm-ZnS buffer and an optimized window layer.

We measured the energy band-gap (E_g) of the 8-nm-thick ZnS film grown on the CIGS. The E_g of the thin ZnS film prepared on the CIGS was obtained by an extrapolation method from the reflection electron-energy-loss spectra (REELS), as shown in Figure 6a. The incident primary electron beam energy (E_0) is proportional to the penetration depth of the ZnS film, which means that the lower E_0 yields the data from shallower depths. The E_g at the near-surface of ZnS film (E_g = 3.40 eV) was slightly lower than inside the film (E_g = 3.56 eV). Both the measured E_gs are much higher than the typically used buffers.[38] The high E_g of 3.40 − 3.56 eV in the ZnS film was allowed to avoid light absorption at high energy irradiation as shown in EQE spectrum (Figure 5c).

We observed SEM and TEM images to characterize the structural property of the ultra-thin ZnS film, as shown in Figures 6b and c. The CIGS film has rough surface morphology because the grains were very large (~ 1 um), which forms deep grain boundaries. We, however, found that the thin ZnS film uniformly covered the CIGS surface. Figure 6c illustrates the TEM image at the ZnO/ZnS/CIGS

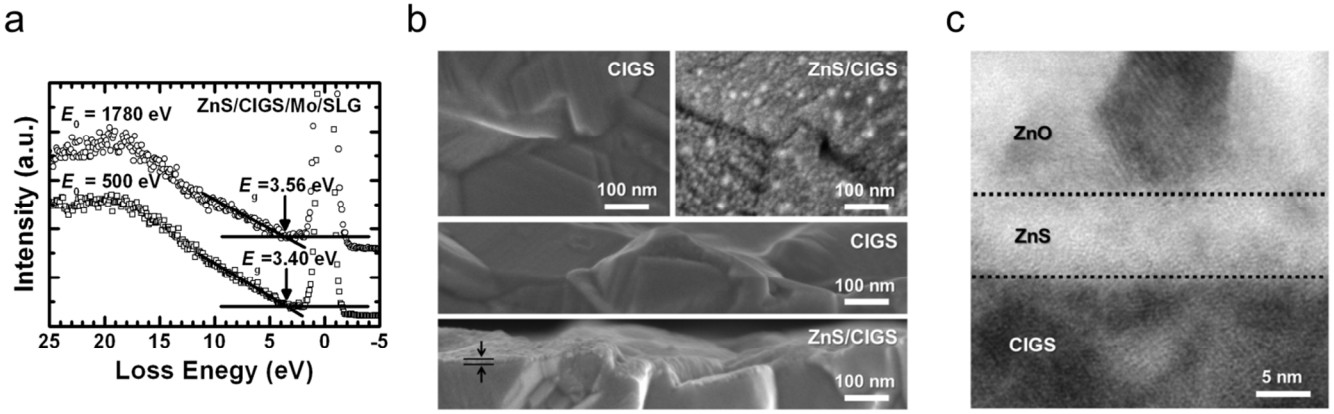

Figure 6. (a) Energy band-gaps obtained by REELS spectra at different incident energies. (b) SEM cross-section and top-view images of ZnS/CIGS and CIGS. (c) TEM cross-section image of ZnO/ZnS/CIGS.

Journal of Materials Chemistry A Accepted Manuscript

interfaces. The ZnS appeared to show an amorphous phase without distinctive crystalline structure, although the ZnO and the CIGS exhibited a columnar structure and a polycrystalline structure, respectively.

The elemental diffusion of the buffer materials into CIGS layer is an important issue. The excessive diffusion of Zn or sulfur is known to change the quality of *p-n* junction and the device performances. In SIMS analysis of the ZnS buffer/CIGS sample, however, the secondary ion intensities of Zn and sulfur rapidly decreased as shown in Figure S2. The Zn intensity decreased to three orders of magnitude at a depth of 130 nm which was shorter than other reported values about 150 nm.[20,39,40] On the other hand, the sulfur intensity also drastically decreased to two orders of magnitude at a depth of 50 nm. The sulfur diffusion into the CIGS layer and formation of $Cu(In,Ga)(Se,S)_2$ phase seemed to be negligible. Therefore, the interface between the ZnS and the CIGS can be clearly defined.

Conclusions

In summary, we proposed a novel method to enhance the sulfur reaction using a thermal cracker cell that enables non-toxic and cost-competitive productions of chalcogenide film with a low thermal budget of substrate heating. The high $T_{C\text{-zone}}$ reduced the substrate temperature, maintaining a high quality of the sulfur-based chalcogenide thin film. As $T_{C\text{-zone}}$ increased, the ZnS phase became dominant with evident grain growth, implying that the thermal energy enhanced the reactivity of sulfur. An ultra-thin ZnS film (~ 8 nm) prepared on the uneven CIGS surface showed conformal coverage with an amorphous phase exhibiting E_g of 3.40 – 3.56 eV. The fabricated ZnS film prepared by the thermal cracker was applied to the CIGS thin-film solar cell as a buffer, and the PCE of 12.6% was obtained. This proposed method of sulfur reaction can contribute to the industry of the optoelectronic devices, offering a low-cost and environment-friendly manufacturing method.

Acknowledgements

This work was supported by the 'New & Renewable Energy' of a Korea Institute of Energy Technology Evaluation and Planning (KETEP) grant funded by the Korean government Ministry Of Trade, Industry & Energy (No. 20119010100010, 20123030010030). The authors also would like to acknowledge the financial support from the R&D Convergence Program of MSIP (Ministry of Science, ICT and Future Planning) and ISTK (Korea Research Council for Industrial Science and Technology) of the Republic of Korea (Grant B551179-12-01-00). The authors also thank S. W. Shin and Prof. J. H. Kim for the support with TEM measurements and Dr. K.-S. Lee for his support in fitting *I-V* curves of the solar cells.

Notes and references

[a] Electronics Telecommunications Research Institute (ETRI), 218 Gajeongno, Yuseong-gu, Daejeon 305-700, Republic of Korea. E-mail: dhcho@etri.re.kr

[b] Department of Solar & Energy Engineering, Cheongju University, 298 Daeseongro, Sangdang-gu, Cheongju, Chungbuk 360-764, Republic of Korea

[c] Department of Physics and Applied Physics, Yonsei University, 50 Yonsei-ro, Seodaemun-gu, Seoul 120-749, Republic of Korea

[d] Samsung SDI, 467 Beonyeong-ro, Seobuk-gu, Cheonan-si, Chungcheongnam-do 331-300, Republic of Korea

[e] Korea University of Science and Technology (UST), 217 Gajeongno, Yuseong-gu, Daejeon 305-350, Republic of Korea

† Electronic Supplementary Information (ESI) available. See DOI: 10.1039/c000000x/

1. Y. Zhao and C. Burda, *Energy Environ. Sci.*, 2012, **5**, 5564.
2. W. Ma, J. M. Luther, H. Zheng, Y. Wu and A. P. Alivisatos, *Nano Lett.*, 2009, **9**, 1699-1703.
3. C. Huang, Y. Chan, F. Liu, D. Tang, J. Yang, Y. Lai, J. Li and Y. Liu, *J. Mater. Chem. A*, 2013, **1**, 5402-5407.
4. D. J. Milliron, D. B. Mitzi, M. Copel and C. E. Murray, *Chem. Mater.*, 2006, **18**, 587-590.
5. S. M. Wood, K. C. Klavetter, A. Heller and C. B. Mullins, *J. Mater. Chem. A*, 2014, **2**, 7238-7243.
6. Y. Fu, N. A. Allsop, S. E. Gledhill, T. Köhler, M. Krüger, R. Sáez-Araoz, U. Blöck, M. C. Lux-Steiner and C.-H. Fischer, *Advanced Energy Materials*, 2011, **1**, 561-564.
7. B. Radisavljevic, A. Radenovic, J. Brivio, V. Giacometti and A. Kis, *Nature Nanotech.*, 2011, **6**, 147-150.
8. Y. Wu, C. Wadia, W. Ma, B. Sadtler and A. P. Alivisatos, *Nano Lett.*, 2008, **8**, 2551-2555.
9. X. Duan, C. Niu, V. Sahi, J. Chen, J. W. Parce, S. Empedocles and J. L. Goldman, *Nature*, 2003, **425**, 274-278.
10. P. Sinsermsuksakul, K. Hartman, S. B. Kim, J. Heo, L. Sun, H. H. Park, R. Chakraborty, T. Buonassisi and R. G. Gordon, *Appl. Phys. Lett.*, 2013, **102**, 053901-053905.
11. D. B. Mitzi, L. L. Kosbar, C. E. Murray, M. Copel and A. Afzali, *Nature*, 2004, **428**, 299-303.
12. K. Kim, G. M. Hanket, T. Huynh and W. N. Shafarman, *J. Appl. Phys.*, 2012, **111**, 0837101-0837108.
13. D. A. R. Barkhouse, O. Gunawan, T. Gokmen, T. K. Todorov and D. B. Mitzi, *Prog. Photovolt: Res. Appl.*, 2012, **20**, 6-11.
14. N. Naghavi, D. Abou-Ras, N. Allsop, N. Barreau, S. Bücheler, A. Ennaoui, C. H. Fischer, C. Guillen, D. Hariskos, J. Herrero, R. Klenk, K. Kushiya, D. Lincot, R. Menner, T. Nakada, C. Platzer-Björkman, S. Spiering, A. Tiwari and T. Törndahl, *Prog. Photovolt: Res. Appl.*, 2010, **18**, 411-433.
15. R. J. Reiffenstein, W. C. Hulbert and S. H. Roth, *Annu. Rev. Pharmacol. Toxicol.*, 1992, **32**, 109-134.
16. R. von Burg and T. Stout, *J. Appl. Toxicol.*, 1991, **11**, 447-450.
17. S. Byungha, W. Kejia, O. Gunawan, K. B. Reuter, S. J. Chey, N. A. Bojarczuk, T. Todorov, D. B. Mitzi and S. Guha, in *37th IEEE Photovoltaic Specialists Conference (PVSC)*, 2011, pp. 002510-002514.
18. B. Shin, O. Gunawan, Y. Zhu, N. A. Bojarczuk, S. J. Chey and S. Guha, *Prog. Photovolt: Res. Appl.*, 2013, **21**, 72-76.
19. D.-H. Cho, K.-S. Lee, Y.-D. Chung, J.-H. Kim, S.-J. Park and J. Kim, *Appl. Phys. Lett.*, 2012, **101**, 0239011-0239014.

Journal of Materials Chemistry A Accepted Manuscript

 This journal is © The Royal Society of Chemistry 2012

20. D.-H. Cho, Y.-D. Chung, K.-S. Lee, N.-M. Park, K.-H. Kim, H.-W. Choi and J. Kim, *Thin Solid Films*, 2012, **520**, 2115-2118.
21. Y.-D. Chung, D.-H. Cho, W.-S. Han, N.-M. Park, K.-S. Lee and J. Kim, *J. Korean Phys. Soc.*, 2010, **57**, 1826-1830.
22. N.-M. Park, H. S. Lee, D.-H. Cho, Y.-D. Chung, K.-H. Kim, K.-S. Lee and J. Kim, *Prog. Photovolt: Res. Appl.*, 2012, **20**, 899-903.
23. N. M. Park, H. S. Lee and J. Kim, *ETRI J.*, 2012, **34**, 779-782.
24. J.-M. Yoon and Y.-S. Cho, JMON, Korea, 2013.
25. H. Rau, T. R. N. Kutty and J. R. F. Guedes De Carvalho, *J. Chem. Thermodynamics*, 1973, **5**, 833-844.
26. R. Zhang, B. Wang, L. Wei, X. Li, Q. Xu, S. Peng, I. Kurash and H. Qian, *Vacuum*, 2012, **86**, 1210-1214.
27. A. Fairbrother, V. Izquierdo-Roca, X. Fontane, M. Ibanez, A. Cabot, E. Saucedo and A. Perez-Rodriguez, *CrystEngComm*, DOI 10.1039/c1033ce42578a.
28. L. Vitos, A. V. Ruban, H. L. Skriver and J. Kollár, *Surf. Sci.*, 1998, **411**, 186-202.
29. J. Mizele, J. L. Dandurand and J. Schott, *Surf. Sci.*, 1985, **162**, 830-837.
30. M. Ohring, *Materials Science of Thin Films: Deposition and Structure (Second Edition)*, Academic Press, San Diego, 2002.
31. NIST X-Ray Photoelectron Spectroscopy Database, http://srdata.nist.gov/xps/, (accessed June 2014).
32. M. Bär, A. Ennaoui, J. Klaer, T. Kropp, R. Sáez-Araoz, N. Allsop, I. Lauermann, H.-W. Schock and M. C. Lux-Steiner, *J. Appl. Phys.*, 2006, **99**, 1235031-1235039.
33. J. D. G. Durn, M. C. Guindo and A. V. Delgado, *J. Colloid Interface Sci.*, 1995, **173**, 436-442.
34. D. H. Shin, J. H. Kim, Y. M. Shin, K. H. Yoon, E. A. Al-Ammar and B. T. Ahn, *Prog. Photovolt: Res. Appl.*, 2013, **21**, 217-225.
35. K. S. Lee, Y. D. Chung, N. M. Park, D. H. Cho, K. H. Kim, J. Kim, S. J. Kim, Y. Kim and S. K. Noh, *Journal of the Optical Society of Korea*, 2010, **14**, 321-325.
36. A. Chirilă, S. Buecheler, F. Pianezzi, P. Bloesch, C. Gretener, A. R. Uhl, C. Fella, L. Kranz, J. Perrenoud, S. Seyrling, R. Verma, S. Nishiwaki, Y. E. Romanyuk, G. Bilger and A. N. Tiwari, *Nat. Mater.*, 2011, **10**, 857-861.
37. Y.-D. Chung, D.-H. Cho, H.-W. Choi, S.-J. Park, J.-H. Kim, B.-J. Ahn, J.-H. Song, K.-S. Lee and J. Kim, *J. Vac. Sci. Technol., A*, 2012, **30**, 04D116-111-104D116-116.
38. R. N. Bhattacharya and K. Ramanathan, *Sol. Energy*, 2004, **77**, 679-683.
39. S. Kijima and T. Nakada, *Appl. Phys. Express*, 2008, **1**, 0750021-0750023.
40. J.-H. Wi, W.-J. Lee, D.-H. Cho, W. S. Han, J. H. Yun and Y.-D. Chung, *Phys. Status Solidi A*, 2014, DOI: 10.1002/pssa.201431232.

Journal of Materials Chemistry A Accepted Manuscript